Discrete gust response analysis of SARAS aircraft

Aravind SEENI*,[1]

*Corresponding author
*Department of Aeronautical Engineering, Rajalakshmi Engineering College,
Thandalam, Chennai 602 105, India,
aravindseeni.s@rajalakshmi.edu.in
[1]Centre for Civil Aircraft Design and Development (C-CADD),
National Aerospace Laboratories (CSIR-NAL),
560017 Bangalore, India

DOI: 10.13111/2066-8201.2023.15.3.7

Received: 20 June 2023/ Accepted: 12 July 2023/ Published: September 2023

Abstract: *The objective of this work is to analyze the aerodynamic response of SARAS transport aircraft to a gust condition. A rigid airframe is assumed. The increments in load factors due to vertical gust are calculated for gust gradient distances varying from 30 to 350ft as per Federal Aviation Requirements (FAR) specifications. The variations in the angles of attack due to gust and airplane motion are also studied. This tuned discrete gust analysis includes the effects of unsteady aerodynamics. The analysis is performed considering the aircraft plunge degree of motion (tail-off). The effect of damping due to the tail contribution is also studied.*

Key Words: *gust response analysis, discrete gust, quasi-steady aerodynamics, unsteady aerodynamics, SARAS aircraft*

1. INTRODUCTION

The effects of external influences like atmospheric gusts on aircraft dynamics had been a concern ever since. The sources of atmospheric turbulence may be categorized according to the degree of severity. A typical gust profile is shown in Fig. 1.

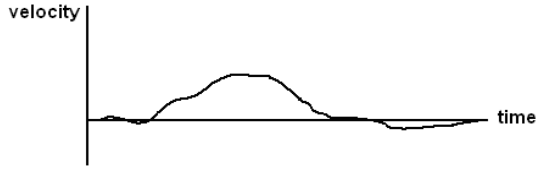

Fig. 1 – Schematic of a discrete gust [1]

Gust profiles tend to be continuous and irregular. Generally, when the profile is continuous, the gust structure is referred to as turbulence. A single pulse is referred to as a gust.

In this paper, the response of a transport aircraft named SARAS to a discrete gust condition is analyzed. Using aircraft dynamic response models, the response to a discrete gust is performed considering quasi-steady and unsteady aerodynamics.

The various models used are explained in Section 2 and the results are presented in Section 3 of this paper. Section 4 provides the analytical validation of obtained numerical results and Section 5 presents the conclusive remarks.

2. AIRCRAFT DYNAMIC RESPONSE MODELS

SARAS specifications

SARAS is a transport category aircraft with a 12+2 seated configuration. The specifications of the aircraft are given in Table 1.

Table 1 – Specifications of SARAS aircraft

Parameter	Value
Maximum take-off weight	7100 kg
Maximum landing weight	6700 kg
Maximum zero-fuel weight	6872 kg
Maximum operating altitude	9 km
Wing area	25.7 m^2
Horizontal tail area	7 m^2
Mean geometric chord	1.904 m
Maximum forward velocity	116.1 m/s

Plunge only equation of motion

If lag in the build-up of lift is neglected, the differential equation for vertical motion can be written as [2]:

$$M\ddot{z} + \frac{\rho}{2}V^2SC_{L_\alpha}\frac{\dot{z}}{V} = \frac{\rho}{2}V^2SC_{L_\alpha}\frac{U(t)}{V} \tag{1}$$

where M is the mass of the airplane, V is the forward speed (TAS), U is the gust velocity (function of time), and Z is the vertical displacement of the airplane. The equation can be simplified to

$$M\ddot{z} + \frac{\rho}{2}VSC_{L_\alpha}\dot{z} = \frac{\rho}{2}VSC_{L_\alpha}U(t) \tag{2}$$

The time lag in a buildup of lft due to airplane motion and gust entry can be modelled using the lift growth "indicial functions": $K_W(t)$ - Wagner function, which accounts for airplane motion and $K_G(t)$ – Kussner function, which accounts for gust entry. The buildup of lift due to an instantaneous change in angle of attack is, $K_w(t) = \frac{C_{L_\alpha}(t)}{C_{L_\alpha}(\infty)}$ and the buildup of lift due to sharp edged gust entry is, $K_G(t) = \frac{C_{L_\alpha}(t)}{C_{L_\alpha}(\infty)}$. To introduce these effects into the differential equation, the changes in angle of attack and gust velocity are assumed to occur in infinitesimal increments. Then, using the Duhamel superposition integral, the equation becomes an integral-differential equation:

$$M\ddot{z} + \frac{\rho}{2}VSC_{L_\alpha}\int_0^t K_w(t-t')\,\ddot{z}(t)dt' = \frac{\rho}{2}VSC_{L_\alpha}\int_0^t K_G(t-t')\,\dot{U}(t')dt' \tag{3}$$

where t' is the infinitesimal steps of time varying from 0 to t and s′ is the infinitesimal steps of chord length varying from 0 to s. For any given airplane, K_W and K_G are functions only of the number of chord lengths travelled, the effect of Mach number, aspect ratio being negligible for conventional subsonic aircraft. As a result, it is desirable to replace t by a non-dimensional time s equal to the number of chord lengths travelled:

$$s = \frac{Vt}{\bar{c}}, \quad t = \frac{\bar{c}s}{V}; \quad \frac{d}{dt} = \frac{V}{\bar{c}}\frac{d}{ds}; \quad \frac{d^2}{dt^2} = \frac{V^2}{\bar{c}^2}\frac{d^2}{ds^2} \tag{4}$$

The differential equation (9) transforms to equation (11) as follows:

$$M\frac{V^2}{\bar{c}^2}\frac{d^2z}{ds^2} + \frac{\rho}{2}VSC_{L_\alpha}\int_0^s K_w(s-s')\frac{V^2}{\bar{c}^2}\frac{d^2z}{ds'^2}\frac{\bar{c}}{V}ds' = \frac{\rho}{2}VSC_{L_\alpha}\int_0^s K_G(s-s')\frac{V}{\bar{c}}\frac{dU}{ds'}\frac{\bar{c}}{V}ds' \tag{5}$$

Multiplying throughout by $\frac{1}{M}\frac{\bar{c}^2}{V^2}$ gives,

$$\frac{d^2z}{ds^2} + \frac{(\rho/2)\bar{c}SC_{L_\alpha}}{M}\int_0^s K_w(s-s')\frac{d^2z}{ds'^2}ds' = \frac{(\rho/2)\bar{c}SC_{L_\alpha}}{M}\frac{\bar{c}}{V}\int_0^s K_G(s-s')\frac{dU}{ds'}ds' \tag{6}$$

Designating by $\frac{1}{\mu}$ as the dimensionless ratio $\frac{\frac{\rho}{2}\bar{c}SC_{L_\alpha}}{M}$, Equation 12 becomes,

$$\frac{d^2z}{ds^2} + \frac{1}{\mu}\int_0^s K_w(s-s')\frac{d^2z}{ds'^2}ds' = \frac{1}{\mu}\frac{\bar{c}}{V}\int_0^s K_G(s-s')\frac{dU}{ds'}ds' \tag{7}$$

The dimensionless parameter is expressed as,

$$\mu = \frac{2M}{\rho\bar{c}SC_{L_\alpha}} \tag{8}$$

is generally referred to as the mass parameter. For design loads determination, the gust profile is considered to be of one-minus-cosine shape, with a gradient distance H:

$$U = \frac{U_{ds}}{2}\left[1 - cos\left(\frac{\pi sc}{H}\right)\right] \tag{9}$$

U_{ds} is the design gust velocity in equivalent airspeed, s is the distance penetrated into the gust in chord lengths.

Transient lift functions

The transient lift functions used for the gust response analysis are as given by Pratt and Walker [4]:

$$K_W = \frac{1}{2\pi}CL_\alpha(s) = 1.000 - 0.165e^{-0.090s} - 0.335e^{-0.600s} \tag{10}$$

$$K_G = \frac{1}{2\pi}CL_\alpha(s) = 1.000 - 0.236e^{-0.116s} - 0.513e^{-0.728s} - 0.171e^{-4.84s} \tag{11}$$

It is noticed that the general form of these equations is

$$\frac{1}{2\pi}CL_g(s) = b_o + b_1 e^{-\beta_1 s} + b_2 e^{-\beta_2 s} + b_3 e^{-\beta_3 s} \tag{12}$$

Solution of the Single Degree of Freedom (1-DOF) gust response equation of motion

The solution is accomplished by a combined analytical-numerical approach as described below. First, Eq. 13 is rewritten to solve for the vertical acceleration as follows:

$$\frac{d^2z}{ds^2} = -\frac{1}{\mu}\int_0^s K_w(s-s')\frac{d^2z}{ds'^2}ds' + \frac{1}{\mu}\frac{\bar{c}}{V}\int_0^s K_G(s-s')\frac{dU}{ds'}ds' \tag{13}$$

Now, since the integral for the effective angle of attack due to gust does not contain the dependent variable 'z', it is integrated directly. MATLAB symbolic math toolbox was used to arrive at the expression for the integral, as a function of the chord lengths penetrated:

$$\alpha_g(s) = \frac{b_0}{2}[1 - cos(s/k)] - C1 - C2 - C3 \tag{14}$$

where i = 1, 2, 3…

$$C_i = \frac{2\pi^2 b_i\left[-k\beta_i\, sin(s/k) + cos(s/k) - e^{-\beta_i s}\right]}{\left(G^2{\beta_i}^2 + 4\pi^2\right)} \tag{15}$$

where k = G/ (2π), G is the gust length, chords, b_i, β_i are the coefficients of the transient lift functions.

The integral for the motion induced angle of attack is numerically integrated using the following scheme: At the every i^{th} step of the integration, $'j'$ is allowed to vary from 1 to $'i'$, so that,

$$\int_0^s K_w(s-s')\frac{d^2z}{ds'^2}ds' = \sum_{j=1}^{j=i} K_w(s(i)-s(j))\,\ddot{z}(j-1)\Delta s \tag{16}$$

and subsequently $\ddot{z}(i)$ is evaluated using Eq. 7, at every i^{th}step of the integration. Finally, $\ddot{z}(s)$ is converted to the time domain by multiplying with V_t^2/c^2 .The incremental normal load factor is obtained by dividing the acceleration by 'g'.

Gust and motion-induced angles of attack

By writing

$$\ddot{z}(s) = \frac{qSCL_\alpha}{M}\alpha_e(s) \tag{17}$$

where $\alpha_e(s)$ is the effective angle of attack.

$$\alpha_e(s) = \left(\frac{U_{de}}{V_e}\right)\alpha_g(s) \;+\; \alpha_c(s) \tag{18}$$

where $\alpha_g(s)$ is the effective angle of attack due to gust and $\alpha_c(s)$ is the angle of attack due to aircraft motion (or damping). It can be shown that

$$\alpha_e(t) = -\frac{1}{c}\int_0^s K_w(s-s')\frac{d^2z}{ds'^2}ds' + \frac{U_o}{V}\int_0^s K_G(s-s')\frac{d(U/U_o)}{ds'}ds' \tag{19}$$

Horizontal tail load

The incremental horizontal tail load due to gust is given by the following expression:

$$\Delta L_{tg} = CL_{\alpha t} q S_w \alpha_e(s) \tag{20}$$

where $CL_{\alpha t}$ includes the effect of wing downwash as well.

Two Degree of Freedom (2-DOF) discrete vertical gust analysis

A 2-DOF discrete gust analysis may be developed using the same assumptions as the one-DOF analysis, except the airplane is allowed to pitch during the gust encounter.

The equation of motion in translation may be written as [3]:

$$\ddot{z}(s) = \frac{qS_w}{M}[C_{l\alpha to}\alpha_e(s) + C_{l\alpha t}\alpha_t(s)] \tag{21}$$

The equation of motion in pitch may be written as:

$$\ddot{\theta}(s) = \frac{qS_w}{M}[C_{l\alpha to}\alpha_e(s_t) + C_{l\alpha t}\alpha_t(s_t)] \tag{22}$$

The effective angle of attack due to the gust and damping may be written as:

$$\alpha_e(s) = (U_{de}/V_e)\alpha_g(s) + \alpha_c(s) \tag{23}$$

The above equation represents the gust encounter of the wing and body and the following equation represents the gust encounter with the horizontal tail:

$$\alpha_t(s_t) = (U_{de}/V_e)\alpha_g(s_t) + \alpha_c(s_t) \tag{24}$$

The relationship between the gust penetration at the wing and the horizontal tail is as follows:

$$s_t = s - x_t/c_w \tag{25}$$

The one-minus-cosine shape is defined by the above equations for the gust striking the wing and the horizontal tail:

$$U(s_t)/U = \left[1 - cos\left(\frac{2\pi s_t}{G}\right)\right]/2 \tag{26}$$

The two-DOF analysis is solved using the following equations to obtain the solution of the equations of motion using finite differences for integration:

$$\dot{\theta}_j = \dot{\theta}_{j-1} + \frac{\Delta t\left(\ddot{\theta}_j + \ddot{\theta}_{j-1}\right)}{2}$$
$$\dot{\alpha}_j = \dot{\theta}_j - \ddot{z}_j/V_t \tag{27}$$

The incremental load factor at the airplane centre of gravity is obtained from the following equation:

$$\Delta n_j = \ddot{z}_j/g \tag{28}$$

The various aerodynamic parameters and derivatives are provided below. The Tail-off pitching moment coefficient is expressed as,

$$C_{M\alpha to} = C_{L\alpha to}(dC_M/dC_L + CG - 0.25) \tag{29}$$

where $C_{L\alpha to}$ is the tail-off lift curve slope, and dC_M/dC_L is the slope of the tail-off pitching moment curve.

The horizontal tail coefficients are expressed as,

$$C_{L\alpha t} = L\alpha_s(1 - \varepsilon_\alpha)/(qSw) \tag{30}$$

$$C_{M\alpha t} = (1 - \varepsilon_\alpha)(M\alpha_s - l_t L\alpha_s)/(qSwc_w) \tag{31}$$

where $L\alpha_s$ is the lift of the horizontal tail due to stabilizer angle of attack (lb/deg) and $M\alpha_s$ is the pitching moment of the horizontal tail due to stabilizer angle of attack, about the horizontal pitch reference axis (in.-lb/deg).

The rate derivatives are expressed as,

$$C_{l\dot{\theta}} = C_{L\alpha T} l_t/V_t \tag{32}$$

$$C_{l\dot{\alpha}} = C_{L\alpha T} x_t(1 - \varepsilon_\alpha) \tag{33}$$

$$C_{M\dot{\theta}} = -C_{L\dot{\theta}} l_t/c_w \tag{34}$$

$$C_{M\dot{\alpha}} = -C_{L\dot{\alpha}} l_t/c_w \tag{35}$$

Incremental angle of attack of wing

The incremental angle of attack of the wing defined below is obtained directly from Eqn. 23:

$$\Delta\alpha_w = \alpha_e(s) \tag{36}$$

Incremental angle of attack of horizontal tail

The incremental angle of attack of the horizontal tail defined below is obtained from the following equation where the first term is defined by Eqn. 24.

$$\Delta\alpha_t = \alpha_t(s_t) + l_t\dot{\theta}_j/V_t \tag{37}$$

Incremental tail loads

Horizontal tail incremental loads may now be calculated from the following equation using the angle of attack of the horizontal tail as defined by the above equation:

$$\Delta L_t = L\alpha_s \Delta L\alpha_t \tag{38}$$

3. DISCRETE GUST RESPONSE: QUASI– STEADY AND UNSTEADY AERODYNAMICS

This study is intended to bring out the effect of including unsteady aerodynamic effects into the analysis of gust response and calculation of gust load factors thereby bringing out its importance from a design point of view. Fig. 2 is a plot of the variation of load factor with time in response to a vertical discrete gust. It is evident that unsteady aerodynamic effects tend to create a lag in the build-up of lift and correspondingly the load factor. This results in the

peak load factor shifting to the right. Furthermore, it is seen that an assumption of quasi-steady aerodynamics gives a peak load factor about 10% higher than in the event including the unsteady effects. This is an important result as it is seen that neglecting unsteady aerodynamic effects is an over-simplification yielding conservative results.

The behaviour of the equations following the peak is also interesting to note. The response is relatively smooth in the unsteady case indicating that the response is more accurate and reflects the real-life gust response better.

Figs. 3 an4 plot the variations of incremental wing loads due to gust and the incremental tail loads due to gust, respectively. The variations are like that of the load factor. Again, it is seen that neglecting the influence of unsteady aerodynamics yields wing and tail loads that are much higher than would be encountered in real life. Thus, it is clear that the inclusion of unsteady aerodynamic effects is mandatory for a more realistic simulation. This study is intended to bring out the effect of including the pitch degree of freedom in addition to the plunge degree of freedom and study the aircraft response to the same.

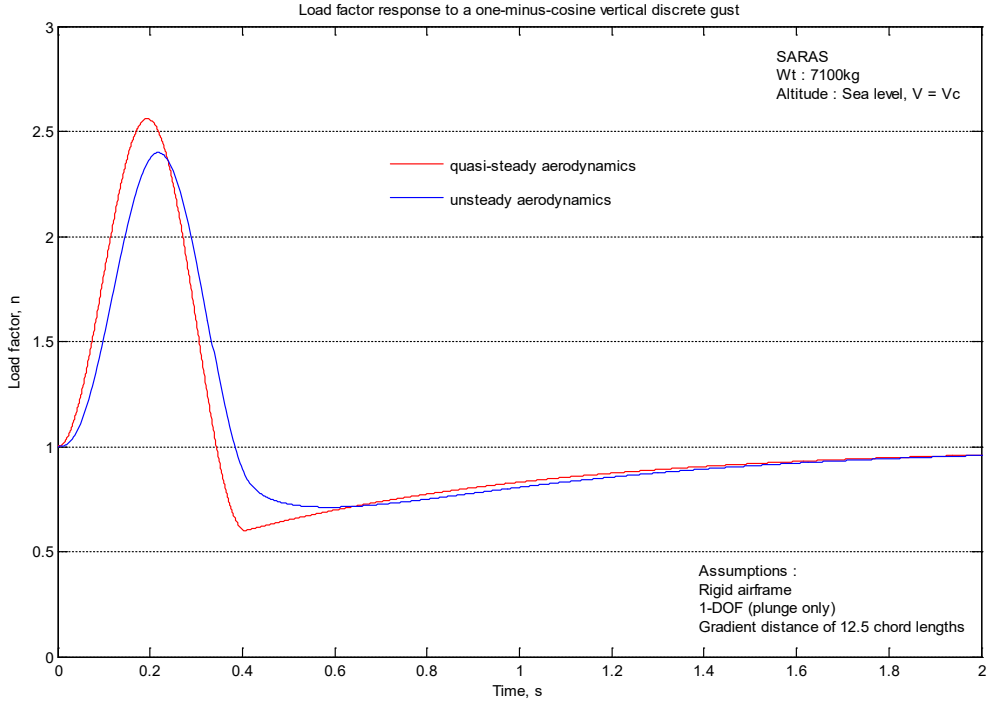

Fig. 2 – Load factor vs. time [1-DOF quasi-steady and unsteady]

Fig. 5 is a plot of the variation of load factor with time in response to a vertical discrete gust. The inclusion of the pitch degree of freedom causes a damped oscillatory response which is as expected. Thus, it is clear that the inclusion of the pitch degree of freedom results in a better estimate of the gust response. However, the important aspect to be noted is that the inclusion of the pitch degree of freedom does not alter the peak load factor much. A very slight reduction of the peak load factor and a slightly earlier occurrence of the peak are observed. Fig. 6 is a plot of the variation of the net angle of attack with time. The plot is similar to that of the variation of load factor. Again, the interesting aspect is the damped oscillatory variation that occurs due to the inclusion of the pitch degree of freedom. This confirms the observation that aircraft executes a damped oscillatory motion on encountering a gust. Changes in peak values are not significant. Fig. 7 is a plot of the variation of incremental tail loads with time

wherein the inclusion of the pitch degree of freedom is compared against the single degree of freedom. While the variation is very similar to that observed in Fig. 3 interesting to note that there is a significant reduction in the peak values. This is due to the pitching velocity of the aircraft which accounts in tail load calculations.

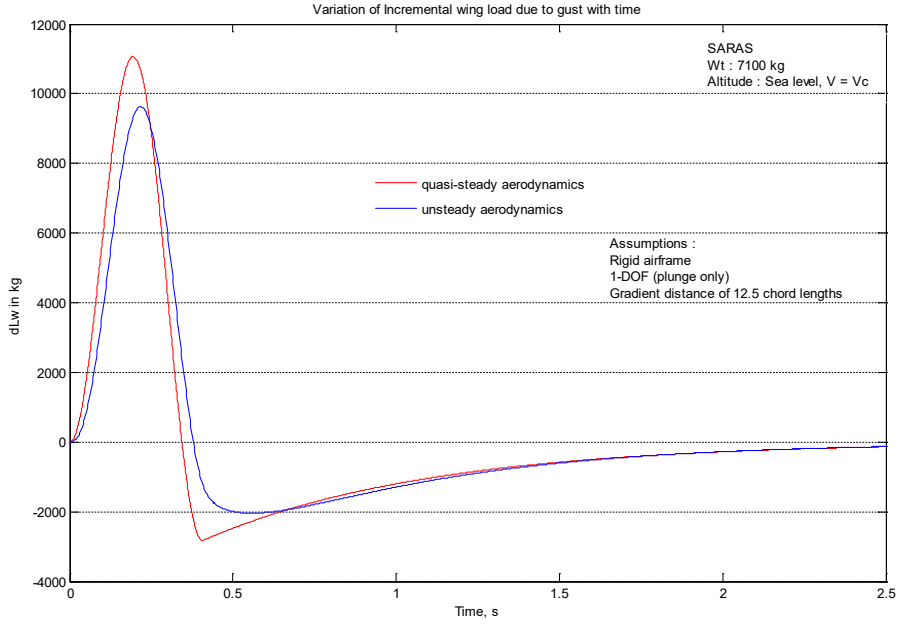

Fig. 3 – Incremental wing loads vs. time [1-DOF quasi-steady and unsteady]

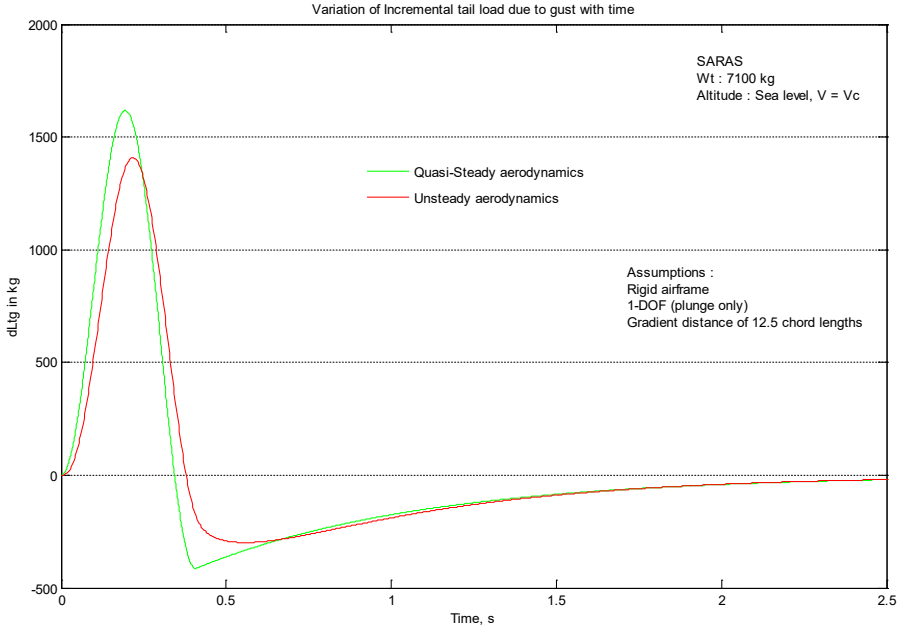

Fig. 4 – Incremental tail loads vs. time [1-DOF quasi-steady and unsteady]

Fig. 8 is a plot of the variations of the angles of attack with time in response to a vertical discrete gust.

While the gust induces a change in the aircraft angle of attack, a corresponding moment produced by the tail dampens this effect by inducing an angle of attack in the opposite direction.

The damping effect develops gradually by which time the gust dies out resulting in a net angle of attack as shown.

Next, the aim is to study the response of the aircraft to vertical discrete gust by tuning the gust gradient distance from 30 to 350 ft and measuring the response of the gust load factors and wing and tail loads.

Fig. 9 is a plot of the variation of load factor with time for various gradient distances varying from 30 ft to 350 ft in step 32.

The interesting thing to note is that for higher gradient distances, the load factor dips further in the negative direction and also takes a longer time to return to normal. The peak load factor is observed at a gradient distance of 167.5 ft.

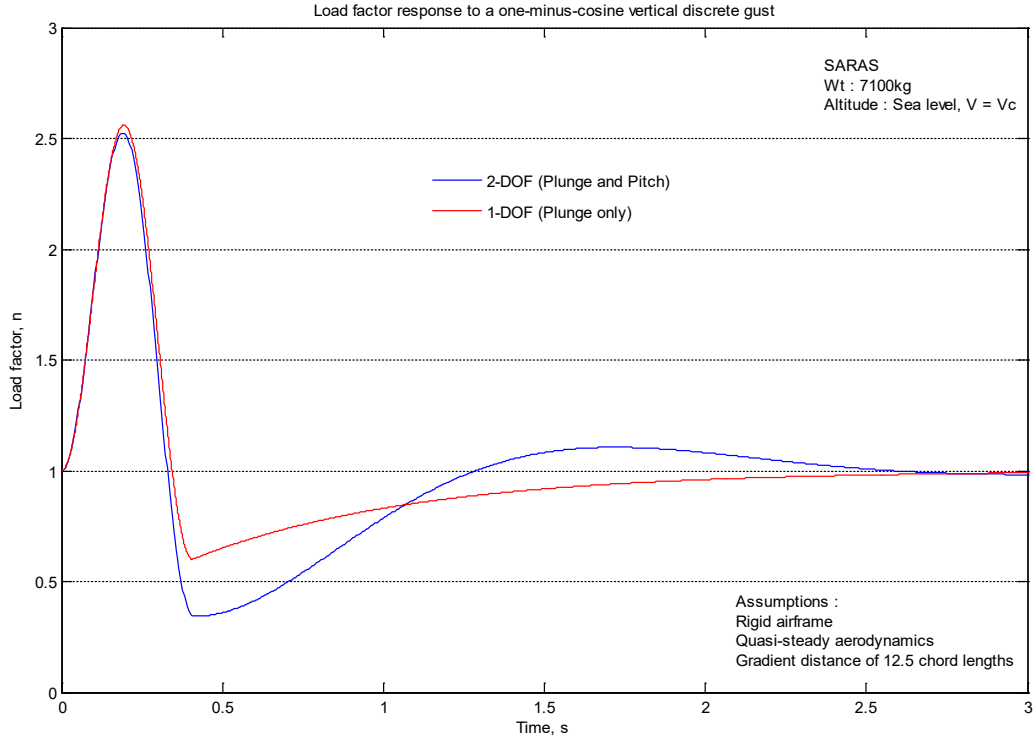

Fig. 5 – Load factor vs. time [1-DOF and 2-DOF quasi-steady]

The variation in peak load factor values which occurs on the inclusion of the second degree of freedom is very minimal as is clear from Fig. 2.

Hence, the study of 2-DOF for unsteady cases is not required. However, study has been performed for the steady case to understand the aircraft's response.

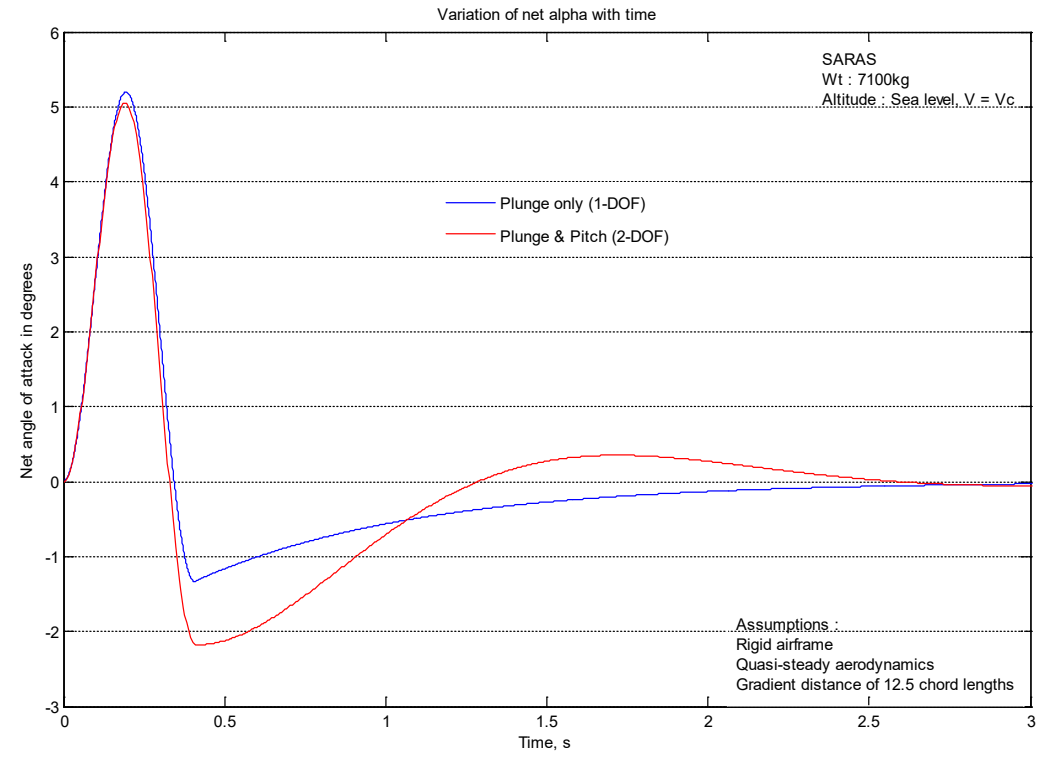

Fig. 6 – The net angle of attack vs. time [1-DOF and 2-DOF quasi-steady]

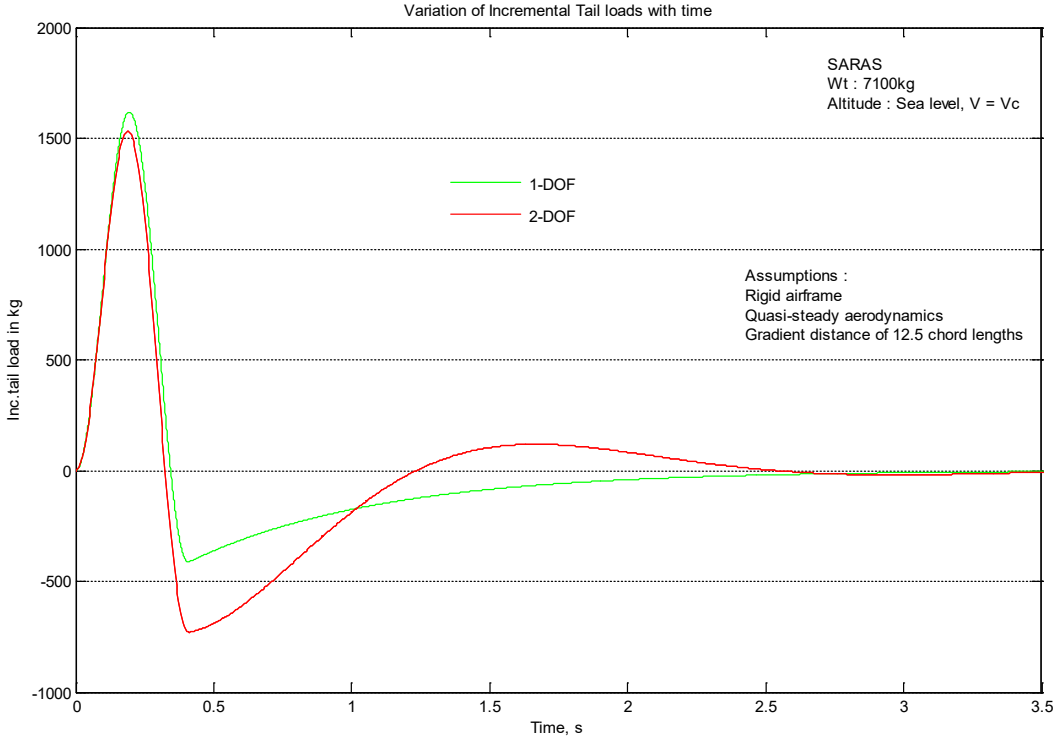

Fig. 7 – Incremental tail load vs. time [1-DOF and 2-DOF quasi-steady]

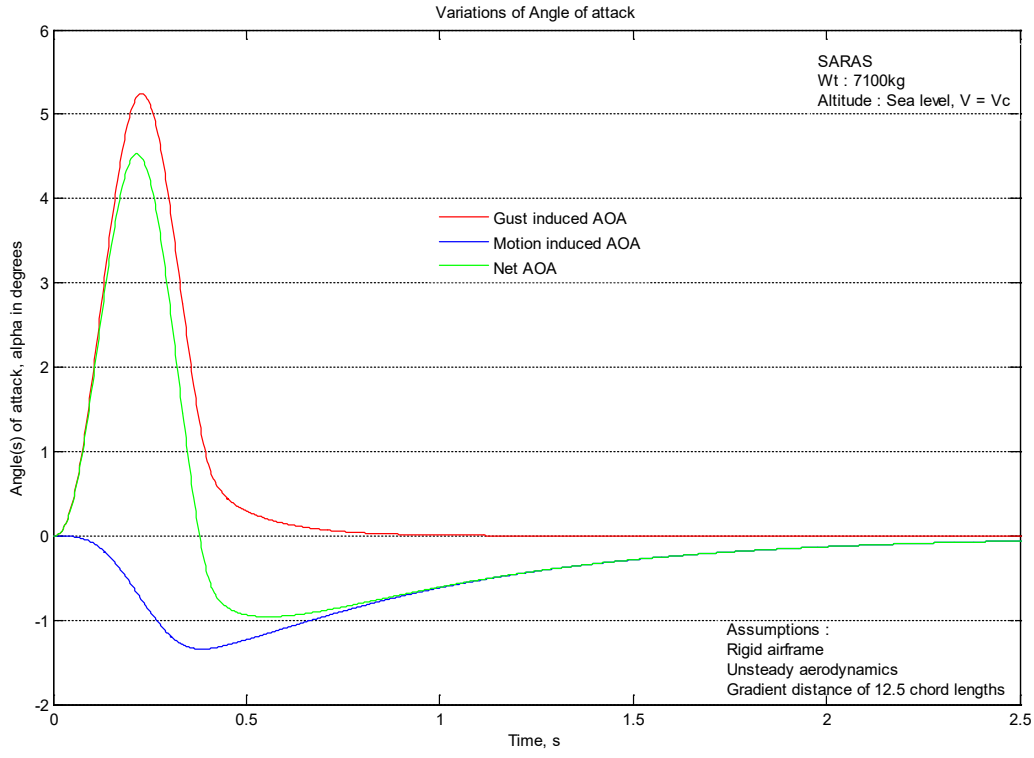

Fig. 8 – Gust, motion and net angle(s) of attack vs. time [1-DOF unsteady]

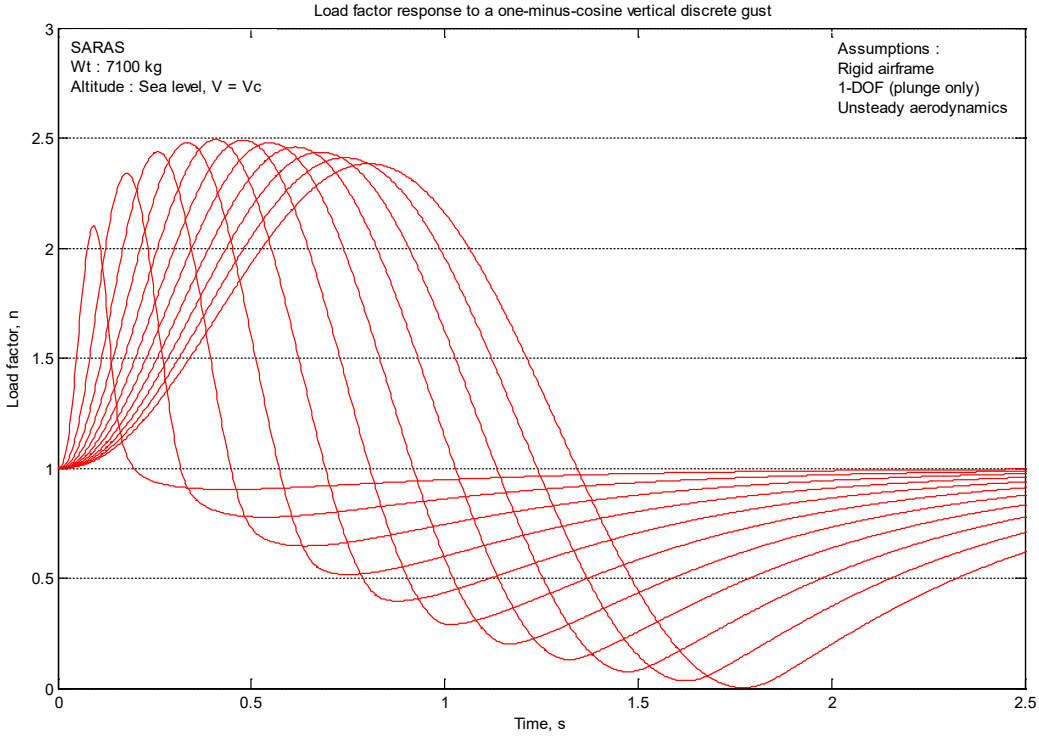

Fig. 9 – Load factor vs. time [1-DOF unsteady]

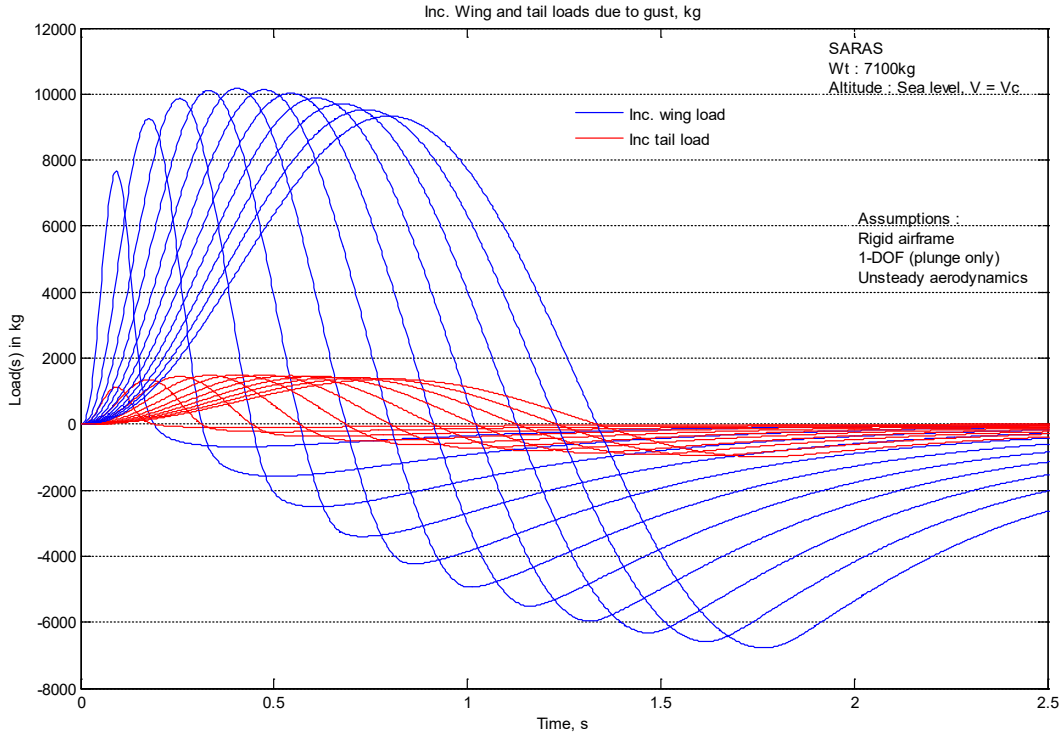

Fig. 10 – Incremental wing and tail load(s) vs. time [1-DOF unsteady]

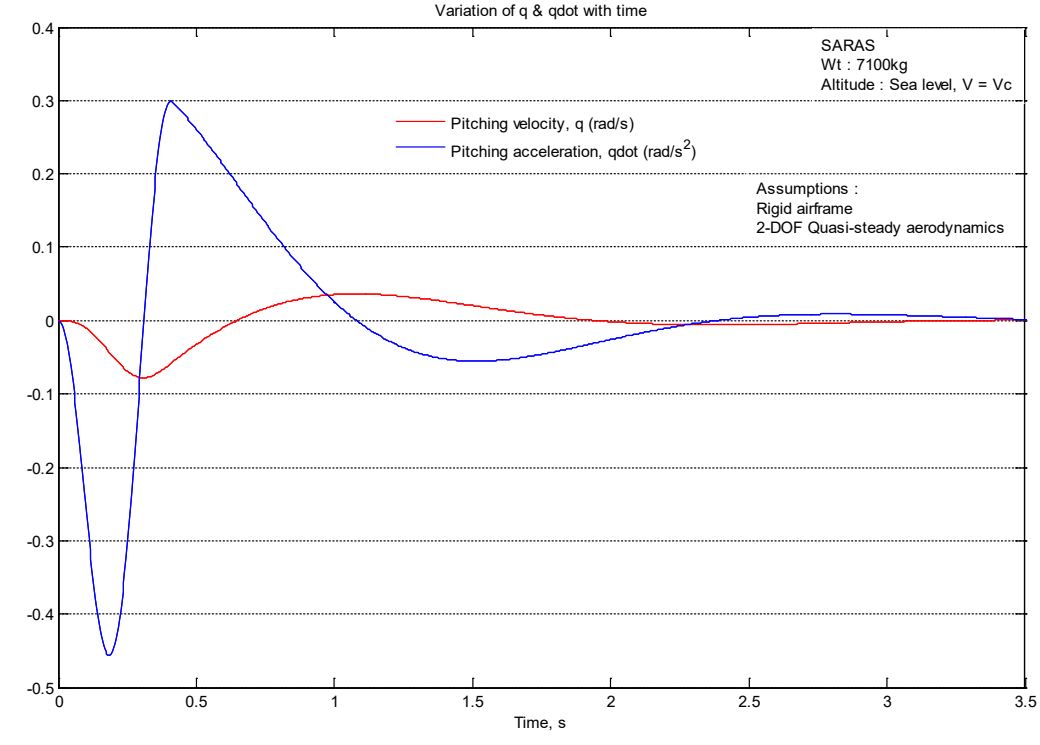

Fig. 11 – Pitching velocity and acceleration vs. time [2-DOF quasi-steady]

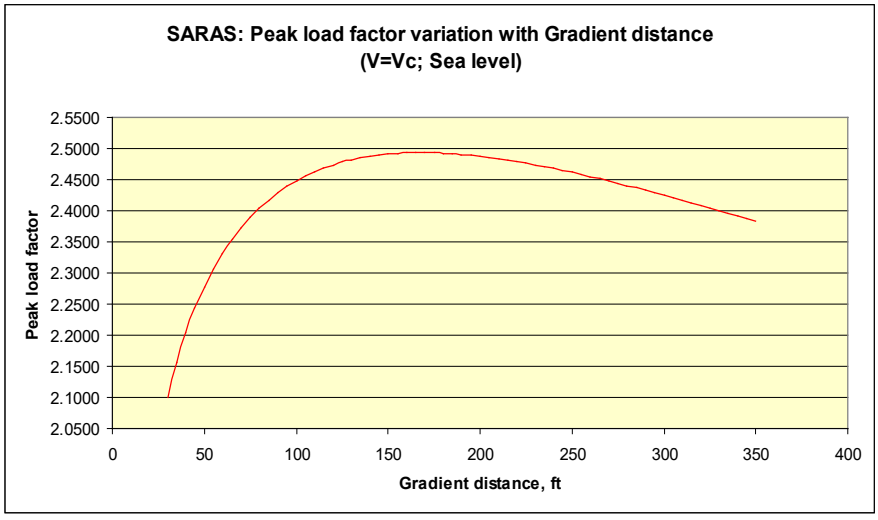

Fig. 12 – Peak load factor vs. Gradient distance [1-DOF unsteady]

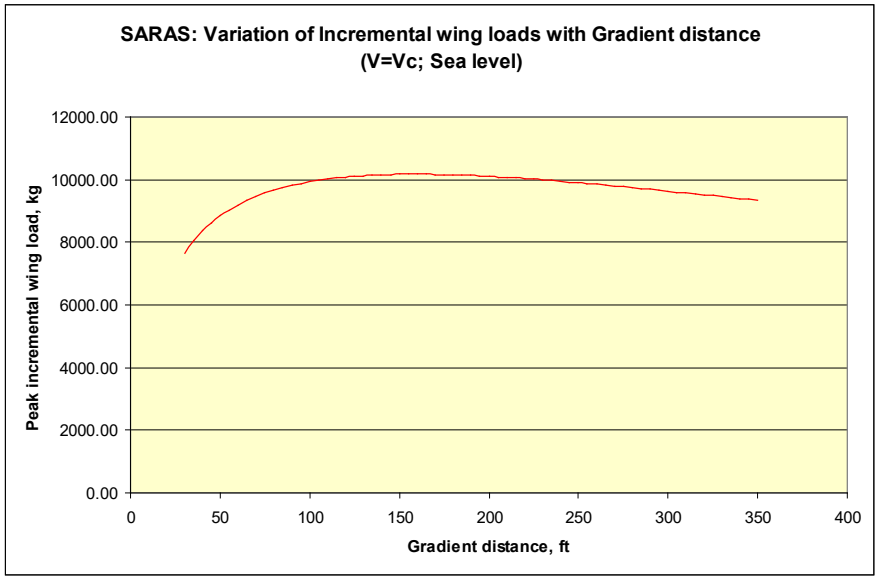

Fig. 13 – Peak incremental wing load vs. Gradient distance [1-DOF unsteady]

Fig. 10 is a plot of the variation of incremental wing and tail loads with time for gradient distances varying from 30 ft to 350 ft in step 32.

The variation is similar to that of the load factor with the peak occurring at about the same gradient distance (167.5 ft).

Fig. 11 is a plot of the variation of pitching velocity and acceleration with time. Figs. 12, 13 and 14 are the plots showing variations of peak load factors, peak incremental wing loads and peak incremental tail loads, respectively considering unsteady aerodynamics.

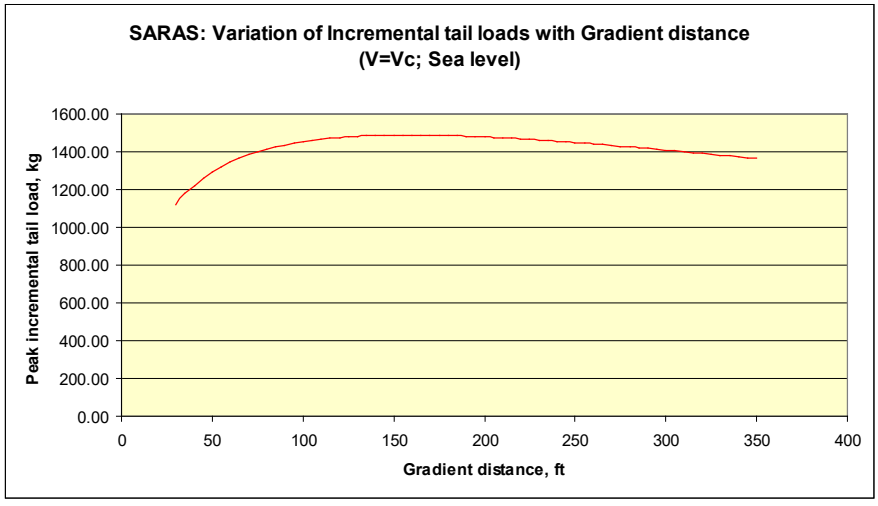

Fig. 14 – Peak incremental tail load vs. Gradient distance [1-DOF unsteady]

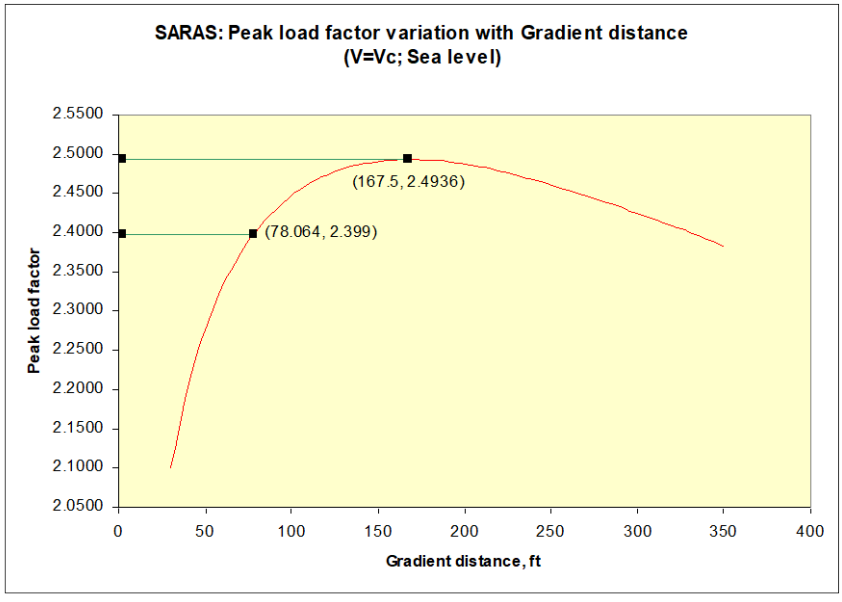

Fig. 15 – Peak load factor vs. Gradient distance [1-DOF unsteady]

4. VALIDATION OF RESULTS

As per FAR specification, the design gust velocity changes with the gradient distance as follows [4]:

$$U_{ds} = U_{ref} F_g \left(\frac{H}{350}\right)^{1/6} \tag{39}$$

Assuming U_{ref} to be 56 fps based on FAR specification [5], we obtain the U_{ds} for $12.5\,\overline{c}$ as follows:

$$H = 12.5\bar{c} \tag{40}$$

For SARAS aircraft, the mean geometric chord length, $\bar{c}$ is 1.904m.

$$H = 12.5 \times 1.904 \times 3.28 = 78.064ft \tag{41}$$

$$U_{ds} = 56 \times 0.9115 \times \left(\frac{78.064}{350}\right)^{1/6} = 39.75ft/s = 12.119m/s \tag{42}$$

The mass factor is calculated from Eq. 15.

$$\mu_g = \frac{2 \times 7100 \times 9.81}{1.2256 \times 1.904 \times 5.63 \times 9.81 \times 25.7} = 42.056 \tag{43}$$

$$K_g = \frac{0.88 \times 42.056}{5.3 + 42.056} = 0.7815 \tag{44}$$

The incremental load factor, Δn is given by the FAR static gust load formula.

$$\Delta \mathrm{n} = K_g \frac{U \mathrm{ds} V C l \alpha}{16.016(W/S)} = \frac{0.7815 \times 12.119 \times 116.1 \times 5.63 \times 25.7}{16.016 \times 7100} \tag{45}$$

$$\Delta n = 1.399$$

$$\text{Load factor, } n = 1+1.399 = 2.399 \tag{46}$$

This research work estimates the aircraft response for vertical discrete gust over a range of gradient distances varying from 30 to 350 ft. Fig. 15 shows the variation of peak load factor for different gradient distances obtained. It is seen that the value of the peak load factor at 12.5 chord lengths obtained from our work agrees perfectly with the value obtained from the static gust load formula.

Traditionally, in the formulation of the FAR static gust load formula, a gust gradient distance of $12.5\bar{c}$ has been assumed and the maximum load factor that is obtained for $12.5\bar{c}$ has been taken into account. However, while tuning the gust gradient distances from 30 ft to 350 ft and plotting the peak load factors against the gradient distances, it is seen that the load factor peaks at 167.5 ft which corresponds to $26.835\bar{c}$. At this gust gradient distance, the peak load factor reaches 2.4936 which is higher than the load factor obtained using FAR static gust load formula.

5. CONCLUSIONS

The discrete gust response analysis of SARAS aircraft is completed.

REFERENCES

[1] L.V. Schmidt, *Introduction to Aircraft Flight Dynamics*, AIAA Education Series, AIAA, Washington DC.
[2] F. M. Hoblit, *Gust Loads on Aircraft: Concepts and Applications*, AIAA Education Series, AIAA, Washington DC, Chaps. 1-3, Appendix A, p. 203.
[3] T. L. Lomax, *Structural Loads Analysis for Commercial Transport Aircraft: Theory and Practice*, AIAA Education Series, AIAA, Washington DC.
[4] K. G. Pratt, and W. G. Walker, *Revised Gust Load Formula and a Re-Evaluation of V-G Data Taken on Civil Transport Airplanes from 1933 to 1950*, NACA Report 1206, Sept.1953.
[5] * * * *Part 25-Airworthiness Standards: Transport Category Airplanes, Federal Aviation Regulations*, U.S. Dept. of Transportation.